


## Detection of Clinically Significant Prostate Cancer Using Micro-Ultrasound vs Magnetic Resonance Imaging/Ultrasound Fusion Biopsy: A Propensity-Weighted Comparative Study

Rafael Castilho Borges , Rafael Rocha Tourinho-Barbosa, Nuno Dias, et al.

Correspondence: Rafael Castilho Borges ([rafa\\_cborges@hotmail.com](mailto:rafa_cborges@hotmail.com)).

Full-length article available at <https://doi.org/10.1097/JU.0000000000004793>.

**Study Need and Importance:** Multiparametric MRI and MRI/ultrasound fusion-guided biopsy (PFB) are widely used for prostate cancer (PCa) diagnosis but remain limited by cost, access, and procedural complexity. Micro-ultrasound-guided biopsy (MB) has recently emerged as a real-time, urologist-operated alternative with lower infrastructure requirements. Whether MB achieves comparable or superior detection of clinically significant PCa (csPCa) relative to PFB remains a critical question for guiding practice, particularly in resource-limited settings.

**What We Found:** We retrospectively analyzed 1119 men with MRI-visible lesions undergoing MB (n = 767) or PFB (n = 352). After inverse probability of treatment weighting, MB showed higher csPCa detection than PFB in combined and systematic biopsies (45% vs 34% and 39% vs 24%, respectively), while targeted cores alone yielded no significant difference (Figure). In the multivariable model, MB and Prostate Imaging-Reporting and Data System 5 lesions were independent predictors of csPCa. Among biopsy-naïve patients, MB also achieved higher overall csPCa detection (49% vs 36%). Furthermore, Gleason upgrading at prostatectomy was significantly less frequent in men diagnosed with MB (17% vs 38%).

**Limitations:** This was a single-center retrospective study, and micro-ultrasound was performed with knowledge of multiparametric MRI results, which may have introduced bias in lesion targeting. Our cohort also included both biopsy-naïve and previ-

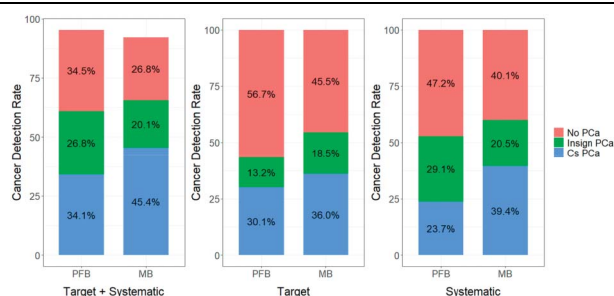



**Figure.** Detection of clinically significant prostate cancer (Cs PCa) with micro-ultrasound (MB) and MRI/ultrasound fusion biopsy (PFB). MB achieved higher Cs PCa detection in systematic and combined biopsies, while targeted cores alone showed no significant difference. Insign PCa indicates clinically insignificant prostate cancer; No PCa, absence of cancer.

ously negative patients, potentially affecting baseline risk profiles. Finally, all MB procedures were performed by highly experienced urologists, which may not reflect outcomes in less specialized settings.

**Interpretation for Patient Care:** Our findings suggest that MB is a feasible and accurate alternative to PFB, particularly where MRI access is limited. By providing higher csPCa yield in systematic and combined strategies, and lower rates of Gleason upgrading, MB may help improve diagnostic accuracy and streamline PCa care. Broader adoption of micro-ultrasound could reduce dependence on costly fusion platforms, increase accessibility, and maintain oncologic safety in diverse clinical environments.

# Detection of Clinically Significant Prostate Cancer Using Micro-Ultrasound vs Magnetic Resonance Imaging/Ultrasound Fusion Biopsy: A Propensity-Weighted Comparative Study

Rafael Castilho Borges <sup>1,2</sup>, Rafael Rocha Tourinho-Barbosa,<sup>3</sup> Nuno Dias,<sup>1</sup> Gustavo de Barros Pena Ribeiro Paiva,<sup>1</sup> Sidney Glina,<sup>2</sup> Oliver Rojas Claros,<sup>4</sup> Lara Rodríguez Sánchez,<sup>1</sup> François Rozet,<sup>1</sup> Eric Barret,<sup>1</sup> Yann Pierre Barbé,<sup>1</sup> Camille Lanz,<sup>1</sup> Rafael Sanchez-Salas,<sup>5</sup> Xavier Cathelineau,<sup>1</sup> Petr Macek,<sup>1</sup> and Fernando Korkeš<sup>2</sup>

<sup>1</sup>Department of Urology, Institut Mutualiste Montsouris, Paris, France

<sup>2</sup>Department of Urology, Faculdade de Medicina do ABC, São Paulo, Brazil

<sup>3</sup>Instituto D'Or de Pesquisa e Ensino (IDOR), Salvador, Brazil

<sup>4</sup>Department of Urology, Hospital Israelita Albert Einstein, São Paulo, Brazil

<sup>5</sup>Department of Urology, McGill University, Montreal, Quebec, Canada

**Purpose:** We compare the detection rates of clinically significant prostate cancer (csPCa) between cognitively targeted micro-ultrasound-guided biopsy (MB) and MRI/ultrasound fusion-guided biopsy (PFB) in men with MRI-visible lesions.

**Materials and Methods:** We retrospectively analyzed 1119 men who underwent MB (n = 767) or PFB (n = 352) between 2019 and 2022. Inverse probability of treatment weighting based on a logistic regression propensity score was applied to balance baseline characteristics between groups. Weighted logistic regression models were used to compare csPCa detection in the overall cohort and in subgroups of biopsy-naïve men and those with anterior lesions. A separate multivariable logistic regression was performed in the full cohort to identify independent predictors of csPCa. Concordance between biopsy and radical prostatectomy Gleason scores was also evaluated.

**Results:** After inverse probability of treatment weighting adjustment, csPCa detection with MB was higher than with PFB in combined sampling (45% vs 34%; odds ratio, 1.61; 95% CI: 1.23-2.11;  $P < .01$ ). However, no significant difference was observed between techniques for targeted biopsies alone, both in the

Submitted February 10, 2025; accepted September 23, 2025; published September 26, 2025.

**Funding/Support:** The Authors have not received funding.

**Conflict of Interest Disclosures:** The Authors have no conflicts of interest to disclose.

**Ethics Statement:** In lieu of a formal ethics committee, the principles of the Helsinki Declaration were followed. All human subjects provided written informed consent with guarantees of confidentiality.

**Author Contributions:**

*Conception and design:* Dias, Rojas Claros, Macek, Borges, Castilho Borges, Tourinho-Barbosa.

*Data acquisition:* Barret, Paiva, Sánchez, Dias, Rojas Claros, Borges, Castilho Borges, Sanchez-Salas, Barbé.

*Data analysis and interpretation:* Lanz, Korkeš, Rozet, Macek, Borges, Castilho Borges, Sanchez-Salas, Tourinho-Barbosa, Glina, Cathelineau, Barbé.

*Critical revision of the manuscript for scientific and factual content:* Lanz, Barret, Korkeš, Rozet, Paiva, Sánchez, Dias, Macek, Borges, Castilho Borges, Sanchez-Salas, Tourinho-Barbosa, Glina.

*Drafting the manuscript:* Korkeš, Rojas Claros, Borges, Castilho Borges, Cathelineau, Barbé.

*Statistical analysis:* Dias, Borges, Castilho Borges, Tourinho-Barbosa.

*Supervision:* Lanz, Barret, Korkeš, Rozet, Paiva, Sánchez, Macek, Borges, Castilho Borges, Sanchez-Salas, Glina, Cathelineau, Barbé.

**Data Availability:** The datasets generated and analyzed during the current study are not publicly available due to patient privacy and institutional policies, but are available from the corresponding author upon reasonable request.

**Corresponding Author:** Rafael Castilho Borges, MD, Department of Urology, Institut Mutualiste Montsouris, 42, Blvd Jourdan, 75674 Paris, France ([rafa\\_cborges@hotmail.com](mailto:rafa_cborges@hotmail.com)).

overall cohort and among biopsy-naïve men. In patients with anterior lesions, csPCa detection rates were also similar. In the full cohort multivariable model, MB and Prostate Imaging–Reporting and Data System 5 lesions were independently associated with csPCa. Gleason upgrading at prostatectomy was more frequent in the PFB group (38% vs 17%;  $P = .01$ ).

**Conclusions:** While MB demonstrated higher csPCa detection in adjusted analyses, the benefit was not consistent across all settings. Further studies are warranted to determine whether this reflects a methodological advantage or context-dependent factors.

---

**Key Words:** biopsy, detection, MRI, prostate cancer, ultrasound

---

OVER the last few years, multiparametric MRI (mpMRI) has emerged as a key modality for detecting and localizing prostate cancer (PCa). Advances in this modality, as well as in MRI/ultrasound prostate fusion–guided biopsy (PFB) platforms, have greatly improved the ability to visualize and target suspicious lesions with high diagnostic accuracy.<sup>1</sup>

Nevertheless, PFB has several limitations that preclude its broad adoption. Fusion devices are expensive, and biopsy procedures often require considerable time.<sup>2,3</sup> In addition, a second visit for the biopsy requires hospitalization and a general anesthesia procedure. There is also a significant learning curve involved in reliably performing the procedure.<sup>4</sup>

In this scenario, micro-ultrasound–guided biopsy (MB) has the potential to bridge acceptable PCa detection rates with the convenience and accessibility of ultrasound apparatus, thus becoming a promising cost-effective alternative to PFB as an upfront diagnostic tool. Recent reports show similar rates of clinically significant PCa (csPCa) detection.<sup>5,6</sup> However, many involve multicenter designs or small cohorts, with variability in biopsy technique and data collection.<sup>6</sup>

This study aims to compare the detection rates of csPCa between MB performed with cognitive targeting and PFB in patients who had a suspicious prostate lesion on a previous MRI.

## MATERIALS AND METHODS

### Study Population

This was a retrospective study of prospectively collected data from men who underwent biopsy from January 2019 to February 2022 at L’Institut Mutualiste Montsouris. The Institutional Review Board approved the study, and patients provided informed consent.

Biopsies were offered to men at clinical risk for PCa based on PSA and/or abnormal rectal exam. Patients underwent MB or PFB depending on operating room availability, preference for anesthesia technique (local in MB, sedation for PFB), and history of biopsy-related infections. Histopathological evaluation was conducted by 3 independent pathologists unaware of the biopsy technique, minimizing bias in Gleason grading.

Patient demographic, clinical, and pathological data were recorded. CsPCa was defined as a Gleason score (GS)  $\geq 7$ . Prebiopsy cancer risk was estimated using the validated Prostate Biopsy Collaborative Group (PBCG) risk calculator.<sup>7</sup>

Exclusion criteria included absence of MRI-visible lesion, men with prior positive biopsy under active surveillance, and absence of targeted biopsy. Of the 2042 men evaluated during the study period, 1119 met the inclusion criteria and were included in the final analysis.

### MRI Assessment and Biopsy Modalities

All patients had biopsies performed after mpMRI. An experienced radiologist localized target lesions through 1.5 and 3.0T prostate mpMRI, incorporating T2-weighted images, dynamic contrast enhancement, and diffusion-weighted imaging. MpMRI findings were classified according to Prostate Imaging–Reporting and Data System (PI-RADS) v2.

#### *Transperineal PFB*

Transperineal PFB was performed with the Artemis device in the surgical setting. For each modality, targeted biopsies followed by systematic sampling were performed by the same urologist in a single session. Typically, 4 targeted samples were taken from each target for PI-RADS  $\geq 3$  or prostate risk identification using micro-ultrasound (PRI-MUS)  $\geq 3$  lesions in PFB and MB, respectively, and 12 cores in systematic biopsies. Slight technique variations were permitted in cases involving large prostates and large target lesions. All biopsies were performed by 4 staff urologists using a conventional spring-loaded gun and 18-gauge needle.

#### *Transrectal MB*

Transrectal MB was performed on an outpatient basis under local anesthesia using the high-resolution ExactVu system. Urologists were aware of prior mpMRI imaging, and mpMRI lesions were cognitively targeted through micro-ultrasound (MUS) guidance. Additional biopsies were taken from lesions identified by MUS. The operator sampled each target under real-time visualization based on the PRI-MUS protocol.<sup>8</sup> After the targeted biopsies were completed, all patients received 12-core systematic biopsies.

### Outcomes

The primary end point of this study was to compare the detection rates of csPCa (CS CDR) in men who underwent MB or PFB. Secondary outcomes included the detection of PCa of any grade, the cancer detection rates in targeted and systematic biopsies between both approaches, the identification of potential

clinical and demographic confounders that could influence detection, and the evaluation of CS CDRs in key clinical subgroups—namely, biopsy-naïve patients and those with lesions located exclusively in the anterior zone. Finally, we assessed the correlation between biopsy and final pathological GS in men who underwent radical prostatectomy.

### Statistical Analysis

Collected data were reported as medians (IQR) or frequencies and proportions for continuous and categorical variables, respectively. All tests were 2-sided, with a significance level set at  $P$  value  $< .05$ . To address potential confounding and better account for baseline differences between the MB and PFB groups, we applied inverse probability of treatment weighting (IPTW) based on the propensity score.

Propensity scores were estimated using a logistic regression model in which the probability of undergoing MB (vs PFB) was regressed on the following baseline covariates: age, PSA, prostate volume, PI-RADS score, MRI lesion size, PBCG cancer risk, and biopsy-naïve status. Stabilized inverse probability weights were calculated to reduce variance and improve covariate balance between groups.<sup>9</sup> Before weighting, unadjusted comparisons of PCa detection rates were performed in the full cohort using Pearson's  $\chi^2$  test.

Covariate balance before and after weighting was assessed using standardized mean differences (SMDs), with values  $< 0.1$  considered indicative of adequate balance. The SMDs were calculated for all covariates included in the IPTW model, both before and after weighting.

A survey-weighted logistic regression was applied to compare oncologic outcomes—including csPCa and any-grade PCa detection—across targeted, systematic, and combined biopsy strategies. For each outcome, weighted proportions, odds ratios (ORs), 95% CIs, and  $P$  values were reported. No truncation was applied to the IPTW weights because the distribution showed no extreme values that would warrant trimming.

In parallel, we conducted a multivariable logistic regression in the full cohort to explore independent predictors of csPCa, with CS CDR as the response variable. Covariates were selected a priori based on clinical relevance and existing literature. The following variables were included in the model: PBCG cancer risk score, prostate volume, previous negative biopsy, biopsy approach, total number of biopsied cores, total biopsy core length, PI-RADS category, and MRI lesion size. Multicollinearity was assessed using variance inflation factors, and all values were below 2, indicating low correlation among predictors. To improve clinical interpretability, continuous predictors were rescaled: PBCG-estimated cancer risk was modeled per 10% increase and prostate volume per 10 mL increase. Results were reported as ORs with 95% CIs.

In addition, an exploratory analysis was conducted to evaluate overall and csPCa detection rates across PRI-MUS categories within each PI-RADS stratum. The Cochran-Armitage test was applied to assess trends across ordered PRI-MUS groups.

The highest GS found in biopsy (targeted or systematic) was compared with the corresponding radical prostatectomy specimen to assess agreement between biopsy

and surgical pathology. Concordance, upgrading, and downgrading rates were compared between groups using Pearson's  $\chi^2$  test, separately for the highest GS overall, in targeted biopsy, and in systematic biopsy.

All statistical analyses were performed using R (version 4.2.2; R Foundation for Statistical Computing).

### RESULTS

A total of 1119 men were consecutively enrolled in the study (MB:  $n = 767$ ; PFB:  $n = 352$ ). Table 1 presents baseline characteristics before and after IPTW. Before weighting, moderate imbalances were observed in prostate volume and biopsy-naïve status. After IPTW, covariates included in the propensity score model achieved adequate balance, with all SMDs below 0.1. Variables not used in the weighting model, such as the number of biopsy cores and core lengths, are reported for descriptive purposes only, without implications for confounding adjustment or causal inference. Covariate balance is visually depicted in the Love plot (Figure 1).

Overall, PCa was detected in 64% of patients. After IPTW, the detection of csPCa remained higher in the MB group compared with the PFB group for the combined targeted plus systematic approach (45% vs 34%; OR, 1.61; 95% CI: 1.23-2.11;  $P < .01$ ). A similar difference was observed in systematic biopsies (39% vs 24%; OR, 2.09; 95% CI: 1.55-2.81;  $P < .01$ ). By contrast, csPCa detection rates in targeted cores did not differ significantly between the MB and PFB groups (36% vs 30%; OR, 1.31; 95% CI: 0.99-1.73;  $P = .06$ ; Table 2 and Figure 2).

Among patients with anterior lesions ( $n = 216$ ), the detection rates of csPCa were lower than in the overall cohort, with no significant difference between biopsy methods. After IPTW adjustment, csPCa was detected in 34% of patients in the MB group vs 30% in the PFB group (OR, 1.18; 95% CI: 0.64-2.18;  $P = .6$ ), with similar findings in targeted and systematic cores (Table 3).

In biopsy-naïve men, MB resulted in higher overall csPCa detection after IPTW (49% vs 36%; OR, 1.70; 95% CI: 1.26-2.31;  $P < .01$ ; Table 4), with a significantly greater yield in systematic cores (44% vs 26%; OR, 2.17; 95% CI: 1.56-3.01;  $P < .01$ ). In targeted biopsies, detection rates were 38% for MB and 32% for PFB, although this difference was not statistically significant ( $P = .07$ ). Baseline characteristics of biopsy-naïve men are presented in Supplementary Table 1 (<https://www.jurology.com>).

In the multivariable logistic regression model—adjusted for relevant clinical, imaging, and procedural variables—both MB (OR, 2.11; 95% CI: 1.51-2.97;  $P < .01$ ) and a PI-RADS 5 score (OR, 3.31; 95% CI: 2.23-4.97;  $P < .01$ ) emerged as the strongest independent predictors of csPCa detection, alongside other significant covariates (Table 5 and Figure 3).

**Table 1.** Baseline Characteristics Before and After Inverse Probability of Treatment Weighting

| Variable   | Full cohort (n = 1119) |                  |                    | Weighted cohort |                 |                    |
|--|------------------------|------------------|--------------------|-----------------|-----------------|--------------------|
|  | MB (n = 767)           | PFB (n = 352)    | Unweighted SMD     | MB              | PFB             | SMD after IPTW     |
| Age, median (IQR), y                                   | 68 (63-72)             | 67 (63-71)       | 0.007 <sup>a</sup> | 68 (63-72)      | 67 (63-71)      | 0.002 <sup>a</sup> |
| Serum PSA, median (IQR), ng/mL                         | 7.6 (5.7-10.9)         | 7.9 (5.7-11)     | 0.086 <sup>a</sup> | 7.7 (5.8-11)    | 7.6 (5.6-10.5)  | 0.001 <sup>a</sup> |
| PSAd, median (IQR)                                     | 0.15 (0.1-0.22)        | 0.14 (0.09-0.21) | 0.101              | 0.15 (0.1-0.21) | 0.14 (0.1-0.22) | 0.030              |
| Biopsy-naïve status (%)                                | 666 (86.8)             | 265 (75.3)       | 0.298 <sup>a</sup> | 83              | 82              | 0.002 <sup>a</sup> |
| Prostate volume, median (IQR), mL                      | 50 (38-69.5)           | 56.5 (40-80)     | 0.231 <sup>a</sup> | 51 (40-72)      | 52 (40-71)      | 0.009 <sup>a</sup> |
| % Prostate Biopsy Collaborative Group risk score (IQR) | 43 (30-55)             | 41 (28-56)       | 0.015 <sup>a</sup> | 43 (30-55)      | 42 (29-56)      | 0.005 <sup>a</sup> |
| No. PI-RADSv2 (%)                                      |                        |                  | 0.039 <sup>a</sup> |                 |                 | 0.006 <sup>a</sup> |
| 3  | 80 (10.4)              | 35 (9)           |                    | 10              | 11              |                    |
| 4  | 478 (62.3)             | 226 (64.2)       |                    | 63              | 63              |                    |
| 5  | 209 (27.2)             | 91 (25.9)        |                    | 27              | 26              |                    |
| MRI lesion size, median (IQR), mm                      | 11 (8.5-14)            | 11 (8-14)        | 0.060 <sup>a</sup> | 11 (8-14)       | 11 (8-15)       | 0.008 <sup>a</sup> |
| No. of biopsied cores, median (IQR)                    | 16 (16-18)             | 15 (14-16)       | 0.836              | 16 (16-18)      | 15 (14-16)      | 0.812              |
| No. of target cores, median (IQR)                      | 4 (4-5)                | 4 (3-4)          | 0.405              | 4 (4-5)         | 4 (3-4)         | 0.385              |
| No. of systematic cores, median (IQR)                  | 12 (12-12)             | 12 (12-13)       | 0.640              | 12 (12-12)      | 12 (12-12)      | 0.633              |
| Target biopsy length, mm (IQR)                         | 43 (34-54)             | 39 (29-50)       | 0.251              | 42 (34-53)      | 39 (30-50)      | 0.220              |
| Systematic biopsy length, mm (IQR)                     | 116 (93-135.5)         | 118 (96-137)     | 0.130              | 116 (94-136)    | 118 (96-137)    | 0.118              |

Abbreviations: IPTW, inverse probability of treatment weighting; MB, micro-ultrasound-guided biopsy; PFB, MRI/ultrasound fusion-guided biopsy; PSAd, PSA density; PI-RADS, Prostate Imaging Reporting and Data System; SMD, standardized mean differences.

Continuous variables are presented as median (IQR). Categorical variables are shown as absolute numbers and percentages in the full cohort and as weighted estimates only after inverse probability of treatment weighting. After inverse probability of treatment weighting, values represent weighted estimates derived from a pseudo-population; the effective sample size does not correspond to the original number of patients. The effective sample size of the weighted pseudo-population was approximately 1119 for the micro-ultrasound-guided biopsy group and 1117 for the PFB group.

<sup>a</sup> Variable included in the inverse probability of treatment weighting model used to estimate propensity scores (age, PSA, prior biopsy, MRI lesion size, prostate volume, Prostate Imaging Reporting and Data System score, and cancer risk). Other variables are reported for descriptive purposes only. Standardized mean differences are shown to evaluate balance before and after weighting, with values < 0.1 indicating adequate balance.

If systematic biopsies had been omitted, 4.0% of csPCa cases in the MB group and 3.0% in the PFB group would have been missed.

### Cancer Rates According to PRI-MUS

Most MUS-detected lesions overlapped with those identified by MRI, with only 24 (3.1%) additional

targets found. Among the lesions identified through MUS, 44% were classified as PRI-MUS 3. The CS CDR increased across the PRI-MUS categories: 36% (PRI-MUS 3), 50% (PRI-MUS 4), and 71% (PRI-MUS 5; Figure 4). Targeted detection rates for csPCa were 32%, 47%, and 66%.

Trend analysis showed a statistically significant increase in csPCa detection across PRI-MUS 3 to 5 within PI-RADS 5 lesions ( $P < .01$ ), but not in PI-RADS 3 ( $P = .8$ ) or 4 ( $P = .3$ ; Supplementary Table 2, <https://www.jurology.com>).

### Biopsy-Surgical Pathology Concordance

Among 156 patients who underwent radical prostatectomy, Gleason upgrading at final pathology was significantly more frequent in the PFB group than in the MB group (38% vs 17%;  $P = .01$ ). When considering targeted biopsies only, concordance rates were similar between groups (MB: 52%; PFB: 52%;  $P = .9$ ), as were upgrading rates (MB: 38%; PFB: 45%;  $P = .5$ ). In contrast, for systematic biopsies, MB demonstrated higher concordance (54% vs 31%;  $P = .02$ ) and lower upgrading rates (35% vs 66%;  $P < .01$ ) compared with PFB (Table 6).

### DISCUSSION

The advent of mpMRI has redefined PCa evaluation, making it a key triage tool for men with suspected disease. Despite guideline inclusion,<sup>10</sup> its widespread use is limited by cost, access, and

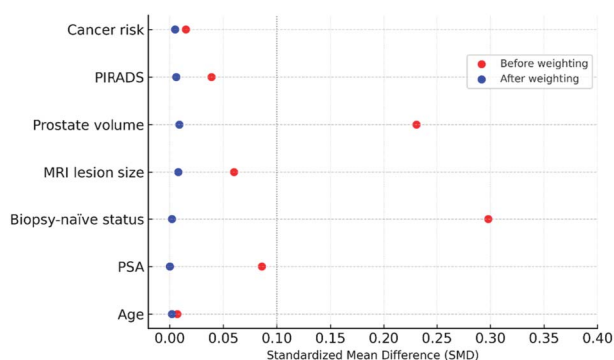


**Figure 1.** Covariate balance before and after inverse probability of treatment weighting. Standardized mean differences for baseline covariates included in the propensity score model are shown before (red) and after (blue) the application of inverse probability of treatment weighting. The model included age, PSA, prostate volume, Prostate Imaging-Reporting and Data System (PIRADS) score, MRI lesion size, biopsy-naïve status, and Prostate Biopsy Collaborative Group-calculated cancer risk. The vertical dashed line at 0.1 denotes the commonly accepted threshold for acceptable covariate balance. Inverse probability of treatment weighting markedly improved balance across all variables.

**Table 2. Prostate Cancer Detection Rate Regardless of Prostate Lesion Location**

| Variable            | Full cohort (n = 1119)                |  |         | Weighted cohort |               |                  |         |
|---------------------|---------------------------------------|--|---------|-----------------|---------------|------------------|---------|
|                     | MB group (n = 767, 68.5%),<br>No. (%) | PFB group (n = 352, 31.5%),<br>No. (%) | P value | MB group (%)    | PFB group (%) | OR (95% CI)      | P value |
| Target + systematic |                                       |  |         |                 |               |                  |         |
| Any PCa             | 516 (67)                              | 203 (58)                               | < .01   | 66              | 61            | 1.22 (0.94-1.59) | .1      |
| CsPCa               | 361 (47)                              | 114 (32)                               | < .01   | 45              | 34            | 1.61 (1.23-2.11) | < .01   |
| Target              |                                       |  |         |                 |               |                  |         |
| Any PCa             | 431 (56)                              | 145 (41)                               | < .01   | 55              | 43            | 1.57 (1.21-2.04) | < .01   |
| CsPCa               | 286 (37)                              | 101 (29)                               | < .01   | 36              | 30            | 1.31 (0.99-1.73) | .06     |
| Systematic          |                                       |  |         |                 |               |                  |         |
| Any PCa             | 474 (62)                              | 173 (49)                               | < .01   | 60              | 53            | 1.34 (1.03-1.73) | .03     |
| CsPCa               | 315 (41)                              | 77 (22)                                | < .01   | 39              | 24            | 2.09 (1.55-2.81) | < .01   |

Abbreviations: CsPCa, clinically significant prostate cancer; MB, micro-ultrasound-guided biopsy; OR, odds ratios; PCa, prostate cancer; PFB, prostate fusion biopsy. Detection rates for any and clinically significant prostate cancer across each biopsy modality, comparing groups before (unadjusted full cohort) and after inverse probability of treatment weighting.

Proportions after inverse probability of treatment weighting represent weighted estimates derived from a reweighted pseudo-population and do not correspond to actual patient counts. The effective sample size of the weighted pseudo-population was approximately 1119 for the MB group and 1117 for the PFB group. Odds ratios, 95% CIs, and P values were calculated using survey-weighted logistic regression models.

For the full (unadjusted) cohort, P values were calculated using Pearson's  $\chi^2$  test, and comparisons reflect the original unadjusted dataset.

End points were assessed separately for overall prostate cancer (Any PCa) and clinically significant prostate cancer, defined as Gleason  $\geq 7$  (International Society of Urological Pathology grade  $\geq 2$ ).

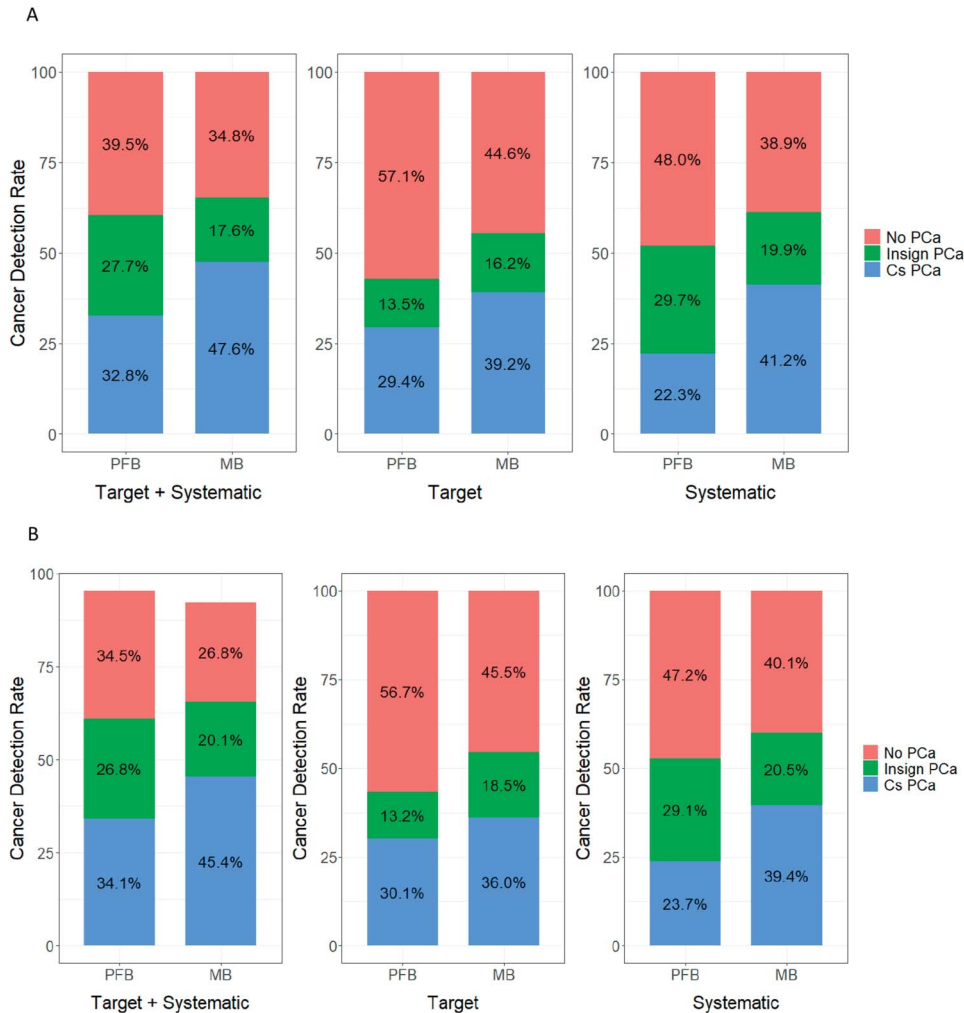


**Figure 2.** Prostate cancer detection rates across biopsy modalities before (A) and after (B) inverse probability of treatment weighting. Stacked bar plots show the distribution of clinically significant prostate cancer (Cs PCa, in blue), clinically insignificant PCa (Insign PCa, in green), and absence of cancer (No PCa, in red). Comparisons are stratified by sampling strategy: Target + Systematic (left), Target only (middle), and Systematic only (right). Panel A presents unadjusted rates from the raw cohort. Panel B presents weighted proportions in the inverse probability of treatment weighting pseudo-population. MB indicates micro-ultrasound-guided biopsy; PFB, prostate fusion biopsy.

**Table 3. Detection Rate of Prostate Cancer in Anteriorly Located Lesions**

| Variable            | Full cohort (n = 216)                 |                                       |         | Weighted cohort |               |                  |         |
|---------------------|---------------------------------------|---------------------------------------|---------|-----------------|---------------|------------------|---------|
|                     | MB group (n = 135, 63.4%),<br>No. (%) | PFB group (n = 81, 36.6%),<br>No. (%) | P value | MB group (%)    | PFB group (%) | OR (95% CI)      | P value |
| Target + systematic |                                       |                                       |         |                 |               |                  |         |
| Any PCa             | 89 (66)                               | 51 (63)                               | .7      | 64              | 66            | 0.91 (0.50-1.64) | .7      |
| CsPCa               | 53 (39)                               | 25 (31)                               | .2      | 34              | 30            | 1.18 (0.64-2.18) | .6      |
| Target              |                                       |                                       |         |                 |               |                  |         |
| Any PCa             | 71 (53)                               | 33 (41)                               | .09     | 50              | 44            | 1.31 (0.74-2.32) | .4      |
| CsPCa               | 43 (32)                               | 23 (28)                               | .6      | 31              | 30            | 1.05 (0.56-1.95) | .9      |
| Systematic          |                                       |                                       |         |                 |               |                  |         |
| Any PCa             | 75 (56)                               | 44 (54)                               | .8      | 54              | 57            | 0.88 (0.51-1.55) | .7      |
| CsPCa               | 41 (30)                               | 16 (20)                               | .08     | 30              | 21            | 1.62 (0.82-3.20) | .2      |

Abbreviations: CsPCa, clinically significant prostate cancer; MB, micro-ultrasound-guided biopsy; PCa, prostate cancer; PFB, prostate fusion biopsy; OR, odds ratios. Detection rates for any and clinically significant prostate cancer across each biopsy modality, comparing groups before (unadjusted full cohort) and after inverse probability of treatment weighting.

Proportions after inverse probability of treatment weighting represent weighted estimates derived from a reweighted pseudo-population and do not correspond to actual patient counts. The effective sample size of the weighted pseudo-population was approximately 217 for the MB group and 214 for the PFB group. Odds ratios, 95% CIs, and P values were calculated using survey-weighted logistic regression models.

For the full (unadjusted) cohort, P values were calculated using Pearson's  $\chi^2$  test, and comparisons reflect the original unadjusted dataset.

End points were assessed separately for overall prostate cancer (Any PCa) and clinically significant prostate cancer, defined as Gleason  $\geq 7$  (International Society of Urological Pathology grade  $\geq 2$ ).

technical complexity.<sup>2</sup> Recently, prostate-specific membrane antigen positron emission tomography/CT has demonstrated promising accuracy in high-risk cases but faces similar adoption barriers.<sup>11</sup>

In this context, MUS has emerged as a more accessible, real-time alternative that urologists can fully operate without the complexity of MRI fusion or nuclear medicine. In our study, following IPTW adjustment, MB demonstrated higher CS CDRs than PFB in systematic and combined biopsies, whereas no significant difference was observed for targeted cores alone. In addition, combined biopsy yielded similar detection rates of any-grade PCa between groups.

Our findings are consistent with prior reports showing comparable diagnostic performance between MUS and MRI-guided techniques.<sup>12-15</sup> Claros

et al<sup>14</sup> compared the detection rates of MUS cognitive-guided biopsies and PFB in 269 patients. The MB showed higher CS CDR than PFB (38% vs 23%;  $P = .02$ ). Similar to our results, when considering overall PCa detection, regardless of GS or random/targeted differentiation, no significant difference was found between groups.<sup>14</sup>

This is further supported by results from the recent OPTIMUM randomized trial, which demonstrated that MB was noninferior to PFB in detecting csPCa. The study reported similar CS CDRs between groups—47.1% for MUS, 42.6% for PFB, and 46.9% for combined MUS/MRI guidance—supporting the diagnostic accuracy of MUS as a viable alternative to MRI-based targeting.<sup>15</sup>

While targeted biopsy enhances lesion-specific detection, systematic sampling—particularly in

**Table 4. Prostate Cancer Detection Rates Among Biopsy-Naïve Men**

| Variable            | Full cohort (n = 931)                 |  |         | Weighted cohort |               |                  |         |
|---------------------|---------------------------------------|--|---------|-----------------|---------------|------------------|---------|
|                     | MB group (n = 666, 71.5%),<br>No. (%) | PFB group (n = 265, 28.5%),<br>No. (%) | P value | MB group (%)    | PFB group (%) | OR (95% CI)      | P value |
| Target + systematic |                                       |  |         |                 |               |                  |         |
| Any PCa             | 467 (70)                              | 160 (60)                               | < .01   | 69              | 65            | 1.28 (0.94-1.73) | .1      |
| CsPCa               | 332 (50)                              | 87 (33)                                | < .01   | 49              | 36            | 1.70 (1.26-2.31) | < .01   |
| Target              |                                       |  |         |                 |               |                  |         |
| Any PCa             | 389 (58)                              | 112 (42)                               | < .01   | 57              | 46            | 1.62 (1.21-2.18) | < .01   |
| CsPCa               | 260 (39)                              | 76 (29)                                | < .01   | 38              | 32            | 1.34 (0.98-1.83) | .07     |
| Systematic          |                                       |  |         |                 |               |                  |         |
| Any PCa             | 435 (65)                              | 139 (53)                               | < .01   | 64              | 57            | 1.40 (1.04-1.88) | .03     |
| CsPCa               | 297 (45)                              | 63 (24)                                | < .01   | 44              | 26            | 2.17 (1.56-3.01) | < .01   |

Abbreviations: CsPCa, clinically significant prostate cancer; MB, micro-ultrasound-guided biopsy; OR, odds ratios; PCa, prostate cancer; PFB, prostate fusion biopsy. Detection rates for any and clinically significant prostate cancer across each biopsy modality, comparing groups before (unadjusted full cohort) and after inverse probability of treatment weighting.

Proportions after inverse probability of treatment weighting represent weighted estimates derived from a reweighted pseudo-population and do not correspond to actual patient counts. The effective sample size of the weighted pseudo-population was approximately 931 for the MB group and 930 for the PFB group. Odds ratios, 95% CIs, and P values were calculated using survey-weighted logistic regression models.

For the full (unadjusted) cohort, P values were calculated using Pearson's  $\chi^2$  test, and comparisons reflect the original unadjusted dataset.

End points were assessed separately for overall prostate cancer (Any PCa) and clinically significant prostate cancer, defined as Gleason  $\geq 7$  (International Society of Urological Pathology grade  $\geq 2$ ).

**Table 5.** Multivariable Logistic Regression Model for Clinically Significant Prostate Cancer Detection

| Covariate                   | Odds ratio | 95% CI    | P value |
|-----------------------------|------------|-----------|---------|
| PBCG cancer risk            | 1.49       | 1.37-1.63 | < .01   |
| Prostate volume             | 0.79       | 0.75-0.83 | < .01   |
| Previous negative biopsy    | 0.89       | 0.59-1.32 | .6      |
| MB                          | 2.11       | 1.51-2.97 | < .01   |
| Total No. of biopsied cores | 1.07       | 0.98-1.16 | .09     |
| Total biopsy core length    | 1.01       | 0.99-1.01 | .3      |
| PI-RADS score               |            |           |         |
| 4                           | 1.30       | 0.98-1.71 | .06     |
| 5                           | 3.31       | 2.23-4.97 | < .01   |
| MRI lesion size             | 1.04       | 1.01-1.07 | .02     |

Abbreviations: MB, micro-ultrasound-guided biopsy; PBCG, Prostate Biopsy Collaborative Group risk calculator; PI-RADS, Prostate Imaging Reporting and Data System.

Odds ratios, 95% CIs, and *P* values are presented for covariates included in the multivariable logistic regression model. Variables were selected a priori based on clinical relevance and prior evidence. The model was performed using the full, unweighted cohort. Continuous variables were rescaled to reflect clinically meaningful changes: Prostate Biopsy Collaborative Group risk per 10% increase and prostate volume per 10 mL increase.

cognitively guided approaches—may increase overall csPCa yield through partial overlap with imaging-suspicious areas.<sup>16-19</sup> Studies have shown that many csPCa detected by systematic cores are located near MRI-visible lesions, suggesting sampling redundancy.<sup>18,19</sup> This overlap may be more common in cognitive approaches, which lack the spatial constraints of software-based fusion.<sup>16,17</sup> In addition, the multifocal nature of PCa and limitations of image-guided targeting may result in missed csPCa outside MRI-visible regions.<sup>20-22</sup> In this context, our higher combined csPCa detection

with MB under IPTW may reflect the complementary contributions of systematic and targeted sampling.

Some previous results have indicated an even higher sensitivity for MB. A multicenter analysis by Klotz et al<sup>5</sup> compared the sensitivity, specificity, positive predictive value, and negative predictive value (NPV) of MB with PFB in 1040 men from 11 sites. Significant PCa was identified in 39% of subjects; MB was noninferior for all 4 metrics and superior in sensitivity (94% vs 90%, *P* = .03) and NPV (85% vs 77%, *P* = .04). The study, however, has some drawbacks, especially methodological differences between sites.

Lughezzani et al<sup>23</sup> compared the diagnostic accuracy of MB and PFB in detecting csPCa in 104 subjects with at least 1 PI-RADS  $\geq$  3 lesion. In total, 54% of patients were diagnosed with PCa, with 34% having csPCa. The sensitivity and NPV were 94% and 90% for MB, respectively. Unlike our selection criteria, the authors included patients with prior positive biopsies, possibly inflating PCa rates.

Indeed, we found broad eligibility criteria across studies, often enrolling men with PCa suspicion, under surveillance, biopsy naïve, or with prior negative biopsies. Similarly, our cohort comprised both biopsy-naïve men and those with a previous negative biopsy, which may introduce selection bias, as biopsy-naïve patients have higher PCa risk.<sup>24</sup> Despite a higher proportion of biopsy-naïve individuals in the MB group, PBCG risk was similar between groups. Moreover, biopsy-naïve status was

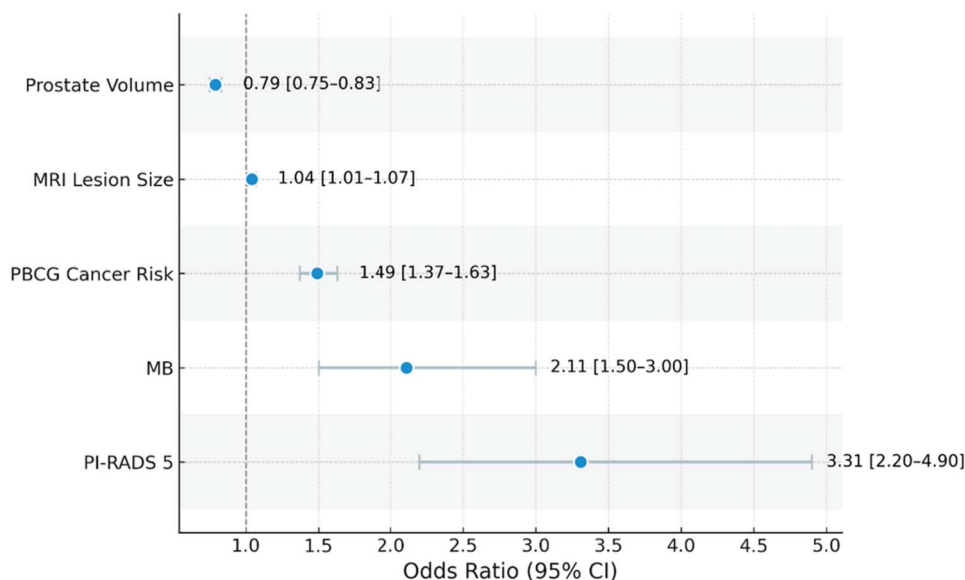


**Figure 3.** Odds ratio plot of multivariate analysis results. Forest plot displaying odds ratios and 95% CIs for predictors of clinically significant prostate cancer detection. Micro-ultrasound-guided biopsy (MB) and Prostate Imaging-Reporting and Data System (PI-RADS) 5 were the covariates most prominently associated with clinically significant prostate cancer detection, based on the magnitude of their odds ratios. The Prostate Biopsy Collaborative Group (PBCG) cancer risk refers to the clinical stratification based on prebiopsy risk factors.

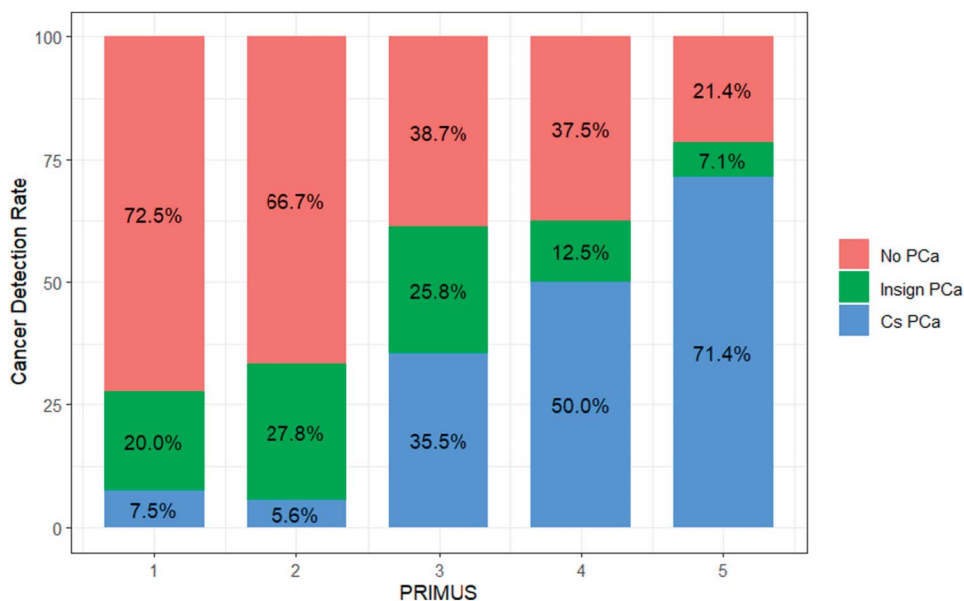


**Figure 4.** Prostate cancer detection rates according to prostate risk identification using micro-ultrasound (PRIMUS) scoring. Stacked bar plot illustrating the distribution of clinically significant prostate cancer (Cs PCa, in blue), clinically insignificant prostate cancer (Insign PCa, in green), and absence of cancer (No PCa, in red) across PRIMUS categories (1-5). A progressive increase in Cs PCa detection is observed with higher PRIMUS scores.

not a significant predictor of csPCa in multivariable analysis. MB and PI-RADS remained the strongest predictors of csPCa detection (Table 5).

Nevertheless, to further explore potential sources of bias and technique-related differences, we conducted a subgroup analysis of biopsy-naïve men and patients with anterior lesions. Among biopsy-naïve men, although targeted csPCa detection was higher in the MB group (38% vs 32%), this difference was not significant ( $P = .07$ ), possibly reflecting subgroup variability.

Similarly, CS CDRs did not differ significantly between groups across targeted, systematic, or combined biopsy strategies in patients with anterior lesions (Table 3). This may reflect a balance of technical factors: while the transperineal approach offers direct access to anterior regions, its longer

needle path can reduce targeting precision. Conversely, transrectal MUS provides real-time, high-resolution imaging, enabling real-time needle adjustment.<sup>8,25</sup> In addition, PFBs are prone to registration errors, particularly in anterior zones.<sup>26</sup> All MB procedures in this study were performed by experienced urologists, likely supporting consistent targeting accuracy.

In a supplementary analysis, we assessed the detection of csPCa across PRI-MUS categories within PI-RADS groups. A significant upward trend appeared only in PI-RADS 5, suggesting a possible role for PRI-MUS in risk stratification among high-risk lesions. However, as PI-RADS 5 lesions are routinely biopsied, its clinical utility remains uncertain. The absence of significance in lower PI-RADS groups may reflect smaller sample sizes,

**Table 6.** Concordance, Upgrading, and Downgrading of Biopsy Gleason Score

|             | Highest GS regardless of SB or TB, No. (%) | <i>P</i> value | Highest GS in TB, No. (%) | <i>P</i> value | Highest GS in SB, No. (%) | <i>P</i> value |
|-------------|--|----------------|---------------------------|----------------|---------------------------|----------------|
| Concordance |  | .2             |                           | .9             |                           | .02            |
| MB          | 85 (67)                                    |                | 66 (52)                   |                | 69 (54)                   |                |
| PFB         | 16 (55)                                    |                | 15 (52)                   |                | 9 (31)                    |                |
| Upgrading   |  | .01            |                           | .5             |                           | < .01          |
| MB          | 22 (17)                                    |                | 48 (38)                   |                | 45 (35)                   |                |
| PFB         | 11 (38)                                    |                | 13 (45)                   |                | 19 (66)                   |                |
| Downgrading |  | .3             |                           | .2             |                           | .2             |
| MB          | 20 (16)                                    |                | 13 (10)                   |                | 13 (10)                   |                |
| PFB         | 2 (6.9)                                    |                | 1 (3.4)                   |                | 1 (3.4)                   |                |

Abbreviations: GS, Gleason score; MB, micro-ultrasound-guided biopsy; PFB, prostate fusion biopsy; SB, systematic biopsy; TB, targeted biopsy. Comparison of concordance, upgrading, and downgrading rates between micro-ultrasound-guided biopsy and MRI/ultrasound fusion-guided biopsy, according to (1) the highest Gleason score detected in either systematic biopsy or targeted biopsy; (2) the highest Gleason score in targeted biopsy; and (3) the highest Gleason score in systematic biopsy. Data are reported as numbers (%), and *P* values were calculated using Pearson's  $\chi^2$  test without continuity correction (Yates), comparing micro-ultrasound-guided biopsy and prostate fusion biopsy groups for each classification.

particularly for PI-RADS 3, which is likely a result of our center's referral pattern, where patients with higher clinical suspicion are more commonly evaluated. Further prospective studies are needed to confirm these findings.

To the best of our knowledge, this is the first study comparing biopsy results with the gold standard of surgical pathology. Despite the limited number of specimens available, our report indicates a significantly lower upgrading rate in men who underwent MB compared with PFB (17% vs 38%;  $P < .01$ ; Table 6).

Our study has several limitations. First, MUS images were not interpreted without the knowledge of at least 1 PI-RADS  $\geq 3$  lesion on mpMRI. This could introduce a high risk of bias, as the operator might expect a lesion on the ultrasound while targeting the same condition. However, we aimed to compare PCa detection rates in men with suspicious mpMRI results, demonstrating the additional benefit of MB in the well-established diagnostic pathway involving mpMRI.

Although the PBCG risk scores were similar between the groups, the significant differences in the rates of biopsy-naïve men raised concerns about potential selection bias. A subgroup analysis of these patients showed a still significantly higher CS CDR for overall and systematic biopsies, but not for targeted biopsies. Because the professionals were not blinded to the mpMRI images, they were naturally inclined to conduct systematic biopsies close to these areas. This likely contributed to the significant differences observed in CS CDR for these biopsies. To more accurately determine the independent value of MUS images in detecting suspicious lesions, further randomized trials that include blinding to mpMRI are needed.

Finally, another important consideration relates to the professionals performing the procedures. In

our study, both biopsy modalities were carried out by urologists with substantial experience in interventional ultrasonography. This may have contributed to the performance of MB, which relies entirely on real-time image acquisition and interpretation by the operator. By contrast, PFB requires prior MRI segmentation and image registration, often involving radiologists in many institutions. The need for expertise in MRI interpretation and the ability to manage fusion-related technical challenges can introduce variability in diagnostic accuracy, particularly among less experienced practitioners. Indeed, prior studies have shown that operator skill can significantly impact CS CDRs.<sup>27-29</sup> Therefore, our findings reflect not only the intrinsic diagnostic capabilities of each imaging modality but also practical and procedural factors that directly influence their clinical effectiveness. These findings underscore the value of adopting a practical and feasible biopsy strategy for the urological community, especially in settings without access to specialized radiological infrastructure.

## CONCLUSIONS

Although MB was associated with higher overall detection of csPCa, it remains uncertain whether this finding reflects an intrinsic diagnostic advantage or is influenced by contextual factors, such as operator expertise. For targeted biopsies, csPCa detection rates were comparable between techniques in the overall population and across key subgroups, including biopsy-naïve men and those with anterior lesions. Moreover, MB was associated with a lower rate of Gleason upgrading at radical prostatectomy. These results support MB as a viable alternative to PFB, especially in resource-limited settings. Further randomized trials are warranted to validate these results.

## REFERENCES

- Kam J, Yuminaga Y, Kim R, et al. Does magnetic resonance imaging-guided biopsy improve prostate cancer detection? A comparison of systematic, cognitive fusion and ultrasound fusion prostate biopsy. *Prostate Int*. 2018;6(3):88-93. doi:10.1016/j.pnii.2017.10.003
- Lughezzani G, Buffi NM, Lazzeri M. Diagnostic pathway of patients with a clinical suspicion of prostate cancer: does one size fit all?. *Eur Urol*. 2018;74(3):400-401. doi:10.1016/j.eururo.2018.05.013
- Walz J. The "PROMIS" of magnetic resonance imaging cost effectiveness in prostate cancer diagnosis?. *Eur Urol*. 2018;73(1):31-32. doi:10.1016/j.eururo.2017.09.015
- Kasabwala K, Patel N, Cricco-Lizza E, et al. The learning curve for magnetic resonance imaging/ultrasound fusion-guided prostate biopsy. *Eur Urol Oncol*. 2019;2(2):135-140. doi:10.1016/j.euo.2018.07.005
- Klotz L, Lughezzani G, Maffei D, et al. Comparison of micro-ultrasound and multiparametric magnetic resonance imaging for prostate cancer: a multicenter, prospective analysis. *Can Urol Assoc J*. 2021;15(1):E11-E16. doi:10.5489/cuaj.6712
- Sountoulides P, Pyrgidis N, Polyzos SA, et al. Micro-ultrasound-guided vs multiparametric magnetic resonance imaging-targeted biopsy in the detection of prostate cancer: a systematic review and meta-analysis. *J Urol*. 2021;205(5):1254-1262. doi:10.1097/JU.0000000000001639
- Ankerst DP, Straubinger J, Selig K, et al. A contemporary prostate biopsy risk calculator based on multiple heterogeneous cohorts. *Eur Urol*. 2018;74(2):197-203. doi:10.1016/j.eururo.2018.05.003
- Ghai S, Eure G, Fradet V, et al. Assessing cancer risk on novel 29 MHz micro-ultrasound images of the prostate: creation of the micro-ultrasound protocol for prostate risk identification. *J Urol*. 2016;196(2):562-569. doi:10.1016/j.juro.2015.12.093
- Austin PC, Stuart EA. Moving towards best practice when using inverse probability of

- treatment weighting (IPTW) using the propensity score to estimate causal treatment effects in observational studies. *Stat Med*. 2015;34(28):3661-3679. doi:10.1002/sim.6607
10. Mottet N, van den Bergh RCN, Briers E, et al. EAU-EANM-ESTRO-ESUR-SIOG guidelines on prostate cancer-2020 update. Part 1: screening, diagnosis, and local treatment with curative intent. *Eur Urol*. 2021;79(2):243-262. doi:10.1016/j.euro.2020.09.042
  11. Pepe P, Pennisi M. Targeted biopsy in men high risk for prostate cancer: <sup>68</sup>Ga-PSMA PET/CT versus mpMRI. *Clin Genitourin Cancer*. 2023;21(6):639-642. doi:10.1016/j.clgc.2023.06.007
  12. Cornud F, Lefevre A, Flam T, et al. MRI-directed high-frequency (29 MHz) TRUS-guided biopsies: initial results of a single-center study. *Eur Radiol*. 2020;30(9):4838-4846. doi:10.1007/s00330-020-06882-x
  13. Rodriguez Socarras ME, Gomez Rivas J, Cuadros Rivera V, et al. Prostate mapping for cancer diagnosis: the Madrid protocol. Transperineal prostate biopsies using multiparametric magnetic resonance imaging fusion and micro-ultrasound guided biopsies. *J Urol*. 2020;204(4):726-733. doi:10.1097/JU.0000000000001083
  14. Claros OR, Tourinho-Barbosa RR, Fregeville A, et al. Comparison of initial experience with transrectal magnetic resonance imaging cognitive guided micro-ultrasound biopsies versus established transperineal robotic ultrasound magnetic resonance imaging fusion biopsies for prostate cancer. *J Urol*. 2020;203(5):918-925. doi:10.1097/JU.0000000000000692
  15. Kinnaird A, Luger F, Cash H, et al; OPTIMUM Investigators. Microultrasound-guided vs MRI-guided biopsy for prostate cancer diagnosis: the OPTIMUM randomized clinical trial. *JAMA*. 2025;333(19):1679-1687. doi:10.1001/jama.2025.3579
  16. Hung M, Ross AE, Li EV, et al. Prostate cancer detection rate of transperineal prostate biopsy: cognitive vs software fusion, a multicenter analysis. *Urology*. 2024;186:91-97. doi:10.1016/j.urology.2023.11.039
  17. Wegelin O, van Melick HHE, Hooft L, et al. Comparing three different techniques for magnetic resonance imaging-targeted prostate biopsies: a systematic review of in-bore versus magnetic resonance imaging-transrectal ultrasound fusion versus cognitive registration. Is there a preferred technique?. *Eur Urol*. 2017;71(4):517-531. doi:10.1016/j.euro.2016.07.041
  18. Lee AYM, Chen K, Cheng CWS, et al. Intensive sampling of the umbra and penumbra improves clinically significant prostate cancer detection and reduces risk of grade group upgrading at radical prostatectomy. *World J Urol*. 2023;41(8):2265-2271. doi:10.1007/s00345-023-04499-5
  19. Raman AG, Sarma KV, Raman SS, et al. Optimizing spatial biopsy sampling for the detection of prostate cancer. *J Urol*. 2021;206(3):595-603. doi:10.1097/JU.0000000000001832
  20. Ahdoot M, Wilbur AR, Reese SE, et al. MRI-targeted, systematic, and combined biopsy for prostate cancer diagnosis. *N Engl J Med*. 2020;382(10):917-928. doi:10.1056/NEJMoa1910038
  21. Kasivisvanathan V, Rannikko AS, Borghi M, et al; PRECISION Study Group Collaborators. MRI-targeted or standard biopsy for prostate-cancer diagnosis. *N Engl J Med*. 2018;378(19):1767-1777. doi:10.1056/NEJMoa1801993
  22. Rouviere O, Puech P, Renard-Penna R, et al; MRI-FIRST Investigators. Use of prostate systematic and targeted biopsy on the basis of multiparametric MRI in biopsy-naive patients (MRI-FIRST): a prospective, multicentre, paired diagnostic study. *Lancet Oncol*. 2019;20(1):100-109. doi:10.1016/S1470-2045(18)30569-2
  23. Lughezzani G, Saita A, Lazzeri M, et al. Comparison of the diagnostic accuracy of micro-ultrasound and magnetic resonance imaging/ultrasound fusion targeted biopsies for the diagnosis of clinically significant prostate cancer. *Eur Urol Oncol*. 2019;2(3):329-332. doi:10.1016/j.euo.2018.10.001
  24. Patel HD, Koehne EL, Shea SM, et al. Risk of prostate cancer for men with prior negative biopsies undergoing magnetic resonance imaging compared with biopsy-naive men: a prospective evaluation of the PLUM cohort. *Cancer*. 2022;128(1):75-84. doi:10.1002/cncr.33875
  25. Schaer S, Rakauskas A, Dagher J, et al. Assessing cancer risk in the anterior part of the prostate using micro-ultrasound: validation of a novel distinct protocol. *World J Urol*. 2023;41(11):3325-3331. doi:10.1007/s00345-023-04591-w
  26. Hale GR, Czarniecki M, Cheng A, et al. Comparison of elastic and rigid registration during magnetic resonance imaging/ultrasound fusion-guided prostate biopsy: a multi-operator phantom study. *J Urol*. 2018;200(5):1114-1121. doi:10.1016/j.juro.2018.06.028
  27. Venderink W, de Rooij M, Sedelaar JPM, Huisman HJ, Futterer JJ. Elastic versus rigid image registration in magnetic resonance imaging-transrectal ultrasound fusion prostate biopsy: a systematic review and meta-analysis. *Eur Urol Focus*. 2018;4(2):219-227. doi:10.1016/j.euf.2016.07.003
  28. Westhoff N, Siegel F, Peter C, et al. Defining the target prior to prostate fusion biopsy: the effect of MRI reporting on cancer detection. *World J Urol*. 2019;37(2):327-335. doi:10.1007/s00345-018-2400-x
  29. Stabile A, Dell'Oglio P, Gandaglia G, et al. Not all multiparametric magnetic resonance imaging-targeted biopsies are equal: the impact of the type of approach and operator expertise on the detection of clinically significant prostate cancer. *Eur Urol Oncol*. 2018;1(2):120-128. doi:10.1016/j.euo.2018.02.002